Neuropsychiatric Disease and Treatment

Dovepress
Taylor & Francis Group

Open Access Full Text Article

ORIGINAL RESEARCH

Exploring the Morphological Study of the Brain in Patients with Bipolar Disorder Based on Structural Magnetic Resonance Imaging

Jiayue Chen[1,2,*], Hongjun Tian[2,*], Xinxin Zhang[3,*], Yingchao Song[4], Yanmin Peng[5], Guotao Yin[6], Qianchen Li[7], Xiaoxiao Xiao[5], Yu Zhang[8], Jun Chen[1], Chuanjun Zhuo[9]

[1]Clinical Research Center, Shanghai Mental Health Center, Shanghai Jiao Tong University School of Medicine, Shanghai, People's Republic of China; [2]Department of Psychiatry, Tianjin Fourth Center Hospital, The Fourth Central Clinical College, Tianjin Medical University, Nankai University Affiliated Tianjin Fourth Center Hospital, Tianjin, People's Republic of China; [3]Department of Radiology, Tianjin Children's Hospital, Children's Hospital, Tianjin University, Tianjin Key Laboratory of BirthDefects for Prevention and Treatment, Tianjin, People's Republic of China; [4]Department of Pediatric Nephrology and Rheumatism and Immunology, Shandong Provincial Hospital Affiliated to Shandong First Medical University, Jinan, People's Republic of China; [5]School of Medical Technology & School of Medical Imaging & Tianjin Key Laboratory of Functional Imaging, Tianjin Medical University, Tianjin, People's Republic of China; [6]Department of Radiology, Qilu Hospital of Shandong University, Jinan, Shandong, People's Republic of China; [7]Department of Pharmacy, Hebei General Hospital, Shijiazhuang, People's Republic of China; [8]Department of Radiology, Beijing Friendship Hospital, Capital Medical University, Beijing, People's Republic of China; [9]Laboratory of Psychiatric-Neuroimaging-Genetic and Co-Morbidity (Pngc_lab), Tianjin Anding Hospital, Nankai University Affiliated Tianjin Anding Hospital, Tianjin Medical University Affiliated Tianjin Anding Hospital, Tianjin Medical University Affiliated Tianjin Mental Health Center, Tianjin, People's Republic of China

*These authors contributed equally to this work

Correspondence: Jun Chen, Clinical Research Center, Shanghai Mental Health Center, Shanghai Jiao Tong University School of Medicine, No. 600 Wanping South Road, Xuhui District, Shanghai, 200030, People's Republic of China, Email doctorcj2010@gmail.com; Chuanjun Zhuo, Laboratory of Psychiatric-Neuroimaging-Genetic and Co-morbidity (PNGC_Lab), Tianjin Anding Hospital, Nankai University Affiliated Tianjin Anding Hospital, Tianjin Medical University Affiliated Tianjin Anding Hospital, Tianjin Medical University Affiliated Tianjin Mental Health Center, No. 13 Liulin Road, Hexi District, Tianjin, 300222, People's Republic of China, Email chuanjunzhuotjmh@163.com

Purpose: The deformation-based morphometry (DBM) method could precisely detect the brain morphological changes, which has rarely been explored in bipolar disorder (BD) patients. This study utilized DBM to identify the structure of grey matter (GM) and white matter in BD patients, and compared DBM with traditional voxel-based morphometry (VBM) on decoding the abnormal changes within the brain, to provide new insights for the pathophysiological mechanism of BD.

Patients and Methods: Brain structural changes in 67 BD patients and 70 healthy controls (HC) were analyzed using DBM and VBM. The spatial correlations of the two indicators in both hemispheres were calculated, regions with significant differences between BD and HC were analyzed by correlating with clinical variables. Furthermore, support vector machine classification algorithm was utilized to detect the capability of VBM, DBM, and fusing two indicators in diagnosing BD patients.

Results: DBM showed increased volumes in GM region in the insula and pregenual anterior cingulate cortex in BD patients. VBM showed reduction of the grey matter volume (GMV) from the inferior temporal gyrus, hippocampus, inferior frontal gyrus, olfactory cortex, fusiform gyrus, middle temporal gyrus, superior temporal gyrus, middle frontal gyrus, middle cingulate and paracingulate gyri, inferior occipital gyrus, Heschl's gyrus, and dorsolateral superior frontal gyrus. The white matter volume (WMV) from the thalamus, inferior frontal gyrus, pallidum, and anterior cingulum were decreased in BD patients. The spatial correlations of the two indicators in both hemispheres were moderately correlated. Furthermore, the highest classification accuracy of DBM-GM and GMV were 69.34% and 72.42%, respectively, which was further increased to 73.72% after fusing two indicators, indicating fusion as the superior strategy.

Conclusion: Our findings indicated structural abnormalities in multiple brain regions in BD patients using VBM and DBM, with different information obtained. Fusing DBM-GM and GMV significantly improved the classification accuracy, suggesting their potential as neuroimaging markers to assist the diagnosis of BD.

Keywords: bipolar disorder, voxel-based morphometry, deformation-based morphometry, machine learning, multivariate pattern analysis

Received: 6 April 2025
Accepted: 25 August 2025
Published: 11 September 2025

Introduction

Bipolar disorder (BD) is a chronic severe mental disorder, imposing a serious burden due to its early age of onset, high rates of self-harm, and hospitalization.[1,2] Previous studies have reported a 20-fold suicide risk from BD patients compared with the general population,[3–6] and suicide attempt is one of the most important causes of mortality.[7] In addition, the diversity of psychopathological features and clinical performances in BD and many other mental disorders makes its classification, diagnosis, and subsequent appropriate treatment considerably complex.[8] Therefore, exploring specific BD neurobiological markers could potentially benefit the diagnosis and therapeutics for BD patients.

The advance of magnetic resonance imaging (MRI) technology provides a non-invasive approach to study the neuropathophysiological mechanism of BD. Numerous studies explored brain structure changes in BD patients, aiming at finding more accurate imaging predictive indicators, but no more consistent conclusions were reached. In the brain morphological analysis method, compared with the traditional voxel-based morphometry (VBM) method, deformation-based morphometry (DBM) reflects the brain structural differences of different individuals based on the deformation field generated in the process of spatial registration. DBM is more sensitive to the detection of local morphological changes, and the results are less affected by spatial registration.[9] However, to date, most of the studies utilized the VBM method in exploring the abnormal changes in grey matter volume (GMV) and white matter volume (WMV) in BD patients.[10–12] There were extremely limited studies utilizing the DBM method to explore brain structure changes in patients with mental illnesses, which were mainly focusing on schizophrenia and depressive disorders. Volz et al found that the volume of the right putamen was increased, while the volume of the frontal lobe, the temporal lobe, the thalamus, the left cerebellar hemisphere, and the right cerebellar vermis were decreased in schizophrenia patients.[13] Another study showed that compared with the healthy controls (HC), major depressive disorder patients have reduced GMV in the right anterior cingulate cortex, right precentral gyrus, and left paracentral lobule.[14] To the best of our knowledge, there are still no studies on the abnormal morphological changes of grey matter (GM) and white matter (WM) by using the DBM method in BD patients.

It has been indicated that multivariate pattern analysis (MVPA) could detect more information than conventional univariate statistical methods by combining information from many features.[15] Among them, the support vector machine (SVM) classification algorithm has good sensitivity and specificity in the classification diagnosis and prediction of neuropsychiatric diseases, especially suitable for studies with limited sample sizes.[16–21] Salvador et al used different machine learning classification algorithms to explore the classification ability of the model in patients with mental illnesses and HC. The study found that GMV could provide the best classification accuracy, with an average classification accuracy of 75% between schizophrenia patients and HC, 63% between BD patients and HC, and 62% between schizophrenia patients and BD patients.[22] Matsuo et al utilized the SVM classification algorithm to classify the GMV in BD patients, obtaining a preferred classification accuracy rate of 88.1%, with a sensitivity of 92.1%, and a specificity of 73.4% between BD patients and HC.[23] However, those studies have mainly focused on investigating GMV rather than WMV in BD patients. Furthermore, utilizing different morphological analysis methods could extract varied indicators in characterizing the structural features of the cerebral cortex, but most of the current studies only reported the result yielded by a single structural indicator, neglecting the fact that different results could be obtained from different methods. For example, applying different morphological analysis methods to detect the temporal lobe epilepsy-related brain structural changes, different aspects of brain atrophy could be revealed,[9] suggesting that the fusion of multiple methods may further enhance the diagnosis and prediction of the disease. To date, it is still unclear whether fusing morphological indicators obtained by VBM and DBM methods could improve the ability of diagnosis and prediction in BD, which reflected a research gap that should be thoroughly investigated.

Based on the above-mentioned research gaps, this study first used the DBM method to explore the morphological differences in GM and WM between BD patients and HC. Additionally, since VBM and DBM reveal changes in brain structure from different perspectives, this study also analyzed the GMV and WMV in the brain structure of BD patients using VBM, and concluded the similarities and differences between the two methods in exploring the neuropathological and physiological mechanisms of BD patients. Moreover, this study also explored the correlation between brain regions with significant differences in VBM and DBM and clinical variables. Finally, based on the SVM classification algorithm, this study examined the classification and diagnosis ability of VBM and DBM in the GM and WM regions in BD

patients, and further tested whether the classification ability after fusing the two morphological indicators was improved than the single morphological indicator.

Materials and Methods

Subjects

We recruited 67 patients with BD and 70 HC. The HC without personal or family history of mental disorders were recruited by local advertisement. The diagnosis of BD was determined by two experienced psychiatrists based on the structured clinical interview criteria of the Diagnostic and Statistical Manual of Mental Disorders, Fourth Edition, Text Revision (DSM-IV-TR), and could not be diagnosed with other mental disorders following the DSM-IV-TR criteria. All the participants were from the Chinese Han ethnic group and right-handed (age = 16~50). The exclusion criteria for all participants are as follows: (1) a history of organic brain disorder and/or severe physical illness; (2) a history of abuse of psychoactive substances; (3) a history of epilepsy, severe traumatic brain injury, or had ever lost consciousness for more than 5 mins due to other reasons; (4) any contraindications to MRI scanning; (5) pregnancy or lactation; (6) intelligence quotient < 70. Moreover, this study was approved by the Ethics Committee of Tianjin Fourth Central Hospital and conducted following the Helsinki Declaration, participants were enrolled in this study voluntarily and signed the informed consent form either by themselves or by their legal guardians.

Imaging Data Acquisition

The MRI scanning was performed on all participants using an Achieva 3.0T MRI scanner (Philips Healthcare, Netherlands). All participants were required to enter the scanning room to quietly rest for 30 minutes to adapt to the environment prior to MRI scanning. In addition, we communicated with the participants in detail, to remind them to close their eyes, relax, stay awake, try to stay motionless, and not engage in any specific mental activities during the scanning process. Foam pads were used to hold the participant's head to avoid head movement, and earplugs were worn to reduce noise. The imaging parameters for collecting 3D T1 weighted structural images were as follows: repetition time (TR) = 8.2ms, echo time (TE) = 3.8ms, flip angle (FA) = 7°, field of view (FOV) = 256 × 256mm, matrix = 256 × 256, layer thickness = 1mm, layer spacing = 1mm, and number of layers = 188. The scanning time is 250s. All brain imaging data of the participants were subjected to image quality control by experienced radiologists, to guarantee the acquisitioned images had no artifacts or abnormal brain structures before proceeded with subsequent data preprocessing analysis.

Data Processing

VBM

MATLAB 2016b software platform was applied for data processing, the T1 images were converted from the original DICOM format to NIFTI format and then utilized CAT12 (Computational Anatomy Toolbox, http://dbm.neuro.uni-jena.de/cat12) toolkit of SPM12 (Statistical Parametric Mapping, http://www.fil.ion.ucl.ac.uk/spm) software for data preprocessing. The preprocessing process was as follows: Firstly, the high-resolution T1 structural images were segmented into GM, WM, and cerebrospinal fluid based on the tissue probability map; The segmented images were then normalized to the Montreal Neurological Institute (MNI) standard space using the diffeomorphic anatomical registration through exponentiated Lie algebra (DARTEL), with voxel sizes resampled to 1.5mm × 1.5mm × 1.5mm. Subsequently, the normalized GM density and WM density maps were multiplied by the nonlinear deformation parameters in the spatial registration process, to finally yield the modulated GM probability maps (GMV image) and WM probability maps (WMV image). In addition, the total intracranial volume (TIV) of each subject was calculated for subsequent analysis. Finally, we conducted sample homogeneity tests on the standardized images using visual box plots and correlation matrices to ensure the quality of the processed images. After confirming the accuracy of the images, the images were smoothed using a Gaussian smoothing kernel with a full width at half maximum (FWHM) of 8mm × 8mm × 8mm.

DBM

The CAT12 toolkit of SPM12 software was used to segment the image. The image was standardized to the MNI standard space by DARTEL and resampled to the voxel size of 1.5mm × 1.5mm × 1.5mm. Then, based on the deformation field parameters obtained by the above nonlinear registration process, the Jacobian matrix was obtained by calculating the second derivative of

the deformation field, and each Jacobian matrix was the deformation information of each voxel. Finally, the images were spatially smoothed using a Gaussian smoothing kernel with a FWHM of 8mm × 8mm × 8mm.

Univariate Statistical Analysis

The SPSS 24 software was used to analyze the demographic and clinical characteristics of the research subjects, and a normality test was conducted on the continuous variables. The *t*-test was utilized to compare the continuous variables that conformed to a normal distribution, and the data were expressed as mean ± standard deviation. When the continuous variable did not conform to a normal distribution, a non-parametric test (Mann–Whitney *U*-test) was selected, with the data expressed as the median (upper quartile, lower quartile); The comparison of non-continuous variables was performed by the chi-square test, set $P < 0.05$ as the significant difference.

The univariate statistical analysis of image data was performed with a *t*-test by the SPM12 software based on the MATLAB 2016b software platform. To reduce the false positive error, the multiple comparison correction was performed using family-wise error (FWE) at the voxel level ($P < 0.05$, FWE-corrected). Since DBM only measured the total brain volume changes but failed to divide the brain into different tissue types; we used the "Template_4_IXI555_MNI152_GS.nii" image[24] that included voxels with a value > 0.3 in CAT12 software to create a GM mask and WM mask to analyze DBM-GM and DBM-WM. All indicators were analyzed using age and gender as covariates to control for their impacts on the results. In addition, the influence of TIV was considered during the comparison of GMV and WMV of BD patients vs HC. To quantify the similarity in spatial patterns between the results obtained by the two methods, we further used Spearman correlation to calculate the spatial correlation coefficients between GMV and DBM-GM, WMV and DBM-WM statistical maps. Besides, the brain regions with significant differences in the above indicators were also taken as regions of interest, and the average voxel values of each region of interest in all patients were extracted, and correlation analysis was conducted between them and clinical variables.

MVPA

The SVM in MVPANI toolbox[25] was utilized to examine the classification ability of image indicators based on four indicators, including DBM-GM, GMV, DBM-WM, and WMV, to explore whether these indicators could distinguish BD patients from HC. Firstly, the 10-fold cross-validation[24] method was used to randomly divide all subjects into 10 subgroups, both BD patients and HC were ensured to be included in each subgroup. 9 subgroups were set as the training set and the remaining 1 subgroup as the testing set. The above-mentioned training was repeated 10 times to ensure that each subgroup had been set as a testing set once. Each feature was standardized before cross-validation: the values in each row (each row represents one sample) were normalized by transforming all values in each sample to *z* scores with a mean of 0 and a standard deviation (SD) of 1 using the following equation:

$$z_{ij} = \frac{x_{ij} - mean(x_{i.})}{SD(x_{i.})} \text{ for the } i^{th} \text{ row}$$

To attenuate the influence of irrelevant or redundant features and enhance the accuracy of the model in the process of cross-validation, we further performed a feature selection. The specific process was as follows: in each cross-validation process, F-test was conducted on the BD patients' group and HC group in the training set. All features were ranked from highest to lowest according to the F-value. Then, the top 10% features with the highest F-value were selected to train the new classifier using the training data set, and the classifier was tested using the reserved testing set, resulting in the classification accuracy of this cross-validation. Through the above process, the classification accuracy will be obtained in each cross-verification, and the final classification accuracy was the average of the classification accuracy obtained in all cross-verification.

The above-mentioned cycle was repeated, with the number of included features increased by 10% per cycle, till all the features were included, 10 selected feature sets and 10 average classification accuracy were totally generated. The statistical significance of classification accuracy was determined by permutation test, with a significance threshold of $P < 0.05$. Furthermore, we conducted 1000 random permutation tests to obtain 1000 random classification accuracies and then used these 1000 random classification accuracies to construct a null distribution. The *P*-value was the percentage greater than or equal to the actual classification accuracy ($P = 0.001$, i.e., 1/1000). Since 10 independent MVPA analyses were performed in

the above-mentioned feature selection process, the Bonferroni correction method was necessary to further perform multiple comparison corrections on the *P* values obtained from the permutation test ($P < 0.05/10 = 0.005$ was considered statistically significant). In addition, to explore whether VBM and DBM indicators are complementary and whether the information fusion between the two indicators could further improve classification accuracy, we used the voting method to fuse two datasets (GM regions and WM regions calculated by different methods) based on the classification results of DBM-WM and WMV, DBM-GM and GMV. The final classification accuracy was also calculated through data fusion, and the *P*-value of the fused classification accuracy was generated through 1000 permutation tests. Besides obtaining the classification accuracy, we also calculated the receiver operating characteristic (ROC) curve and the corresponding area under the curve (AUC) for each classification.

Results

Demographics

The demographic and clinical variables of the participants were shown as below: BD group (n = 67) contained 30 male and 37 female patients, while HC group (n = 70) had 33 male and 37 female participants ($\chi^2 = 0.077$, $P = 0.781$). The age of participants from BD and HC were 23.34 ± 4.74 and 21.64 ± 5.54 years, respectively (t = 1.926, $P = 0.056$). The duration of illness from BD patients was 9.72 ± 8.23 months, and the age of onset was 22.54 ± 4.93 years. In summary, no significant difference was concluded in gender and age between BD patients and HC ($P > 0.05$).

The Comparison of DBM Between BD Patients and HC

The abnormal brain regions of DBM-GM in BD patients and HC were presented in Figure 1. Briefly, in the GM area, the volume of the left insula (the peak MNI coordinate: −43.5, 13.5, −10.5; the number of voxels = 25; t value = 5.0582; effect size = 0.6629) and pregenual anterior cingulate cortex (the peak MNI coordinate: −1.5, 52.5, −1.5; the number of voxels = 15; t value = 4.6180; effect size = 0.05914) were increased in BD patients compared with the HC ($P < 0.05$, voxel-level FWE-corrected). However, there were no statistically significant differences in DBM-WM between BD patients and HC ($P > 0.05$, voxel-level FWE-corrected).

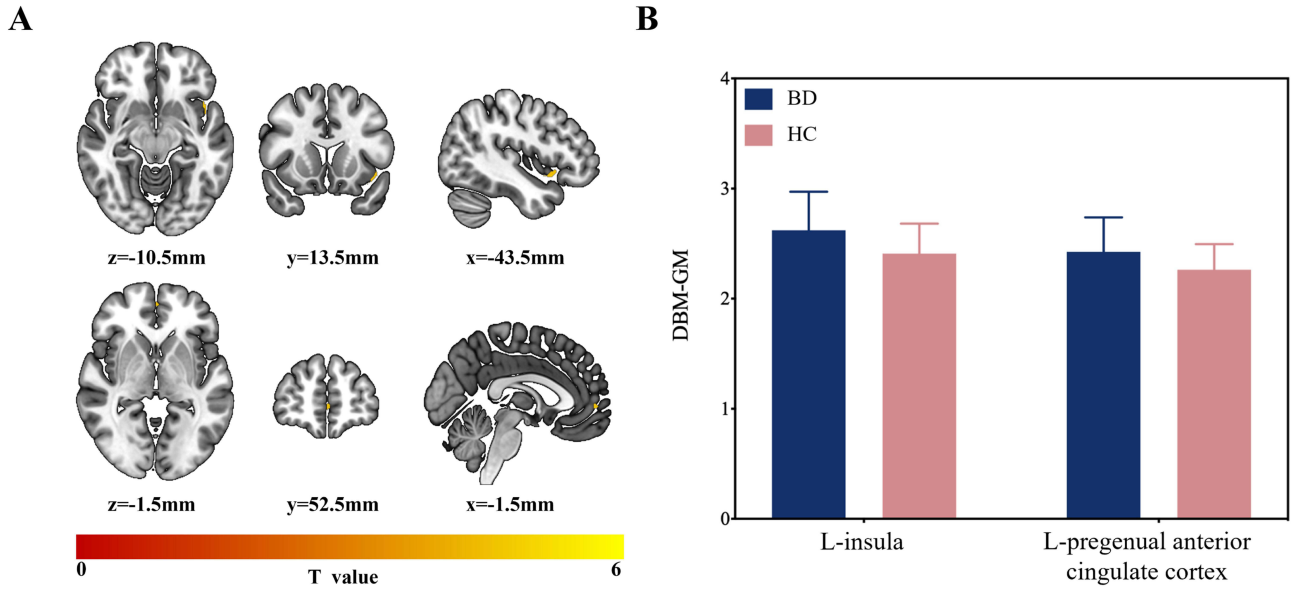

Figure 1 (**A** and **B**), respectively, shows the abnormal brain regions maps and differential changes between bipolar disorder (BD) and healthy controls (HC) in the grey matter (GM) region using the deformation-based morphometry (DBM) method.

https://doi.org/10.2147/NDT.S532650

The Comparison of VBM Between BD Patients and HC

Significant differences of GMV were presented in numerous brain regions between BD patients and HC, as presented in Table 1 and Figure 2. Briefly in BD patients, the GMV from the bilateral inferior temporal gyrus and hippocampus; the left inferior frontal gyrus, olfactory cortex, fusiform gyrus, middle temporal gyrus, superior temporal gyrus, middle frontal gyrus, and middle cingulate and paracingulate gyri; the right inferior occipital gyrus, Heschl's gyrus, and dorsolateral superior frontal gyrus were significantly decreased as compared with HC ($P < 0.05$, voxel-level FWE-corrected).

Similarly, significant differences in WMV were shown in numerous brain regions between BD patients and HC, as shown in Table 2 and Figure 3. BD patients showed significantly decreased WMV in the bilateral thalamus, the right inferior frontal gyrus, the right pallidum, and the right anterior cingulum, as compared with HC ($P < 0.05$, voxel-level FWE-corrected).

The Spatial Correlations of Statistical Maps Between BD Patients and HC Yielded by the VBM and DBM Analysis

Figure 4 showed the spatial correlations between the differences in GMV and DBM-GM, WMV and DBM-WM between BD patients and HC. The pair-wise correlation analyses indicated moderate spatial correlations between GMV and DBM-GM groups ($r = 0.43$ for the left hemisphere and $r = 0.41$ for the right hemisphere, $P < 0.05$); similarly, the spatial correlations between WMV and DBM-WM were also moderate ($r = 0.42$ for the left hemisphere and $r = 0.51$ for the right hemisphere, $P < 0.05$).

Table 1 The Abnormal Brain Regions of GMV in Bipolar Disorder Patients and Healthy Controls

Regions (AAL)	MNI			Number of Voxels	T value	Effect Size
	x	y	z			
L inferior temporal gyrus	−51	−49.5	−18	33	−5.1915	−0.6957
R inferior temporal gyrus	54	−39	−16.5	34	−5.3449	−0.7395
L fusiform gyrus	−24	−33	−16.5	27	−5.1487	−0.6204
R inferior occipital gyrus	37.5	−82.5	−15	51	−5.0966	−0.6988
L hippocampus	−31.5	−13.5	−15	16	−4.8408	−0.6052
L middle temporal gyrus	−61.5	−36	3	1412	−6.1897	−0.8275
L olfactory cortex	0	12	−6	28	−5.0528	−0.6736
L inferior frontal gyrus	−37.5	15	3	42	−5.5819	−0.7255
L superior temporal gyrus	−57	−6	4.5	138	−5.5233	−0.7116
R Heschl's gyrus	48	−9	7.5	109	−5.9209	−0.7156
R hippocampus	27	−36	7.5	56	−6.0424	−0.8233
R dorsolateral superior frontal gyrus	19.5	45	37.5	248	−6.4463	−0.7458
L middle frontal gyrus	−27	31.5	39	27	−5.1186	−0.7897
L middle cingulate and paracingulate gyri	0	−28.5	46.5	58	−5.2569	−0.6983

Notes: T value: the statistic value at the peak voxel within clusters showing significant differences between bipolar disorder patients and healthy controls in the two-sample *t*-test with FWE voxel-level correction.
Abbreviations: GMV, grey matter volume; AAL, anatomical automatic labeling; MNI, Montreal Neurological Coordinate; L, left; R, right.

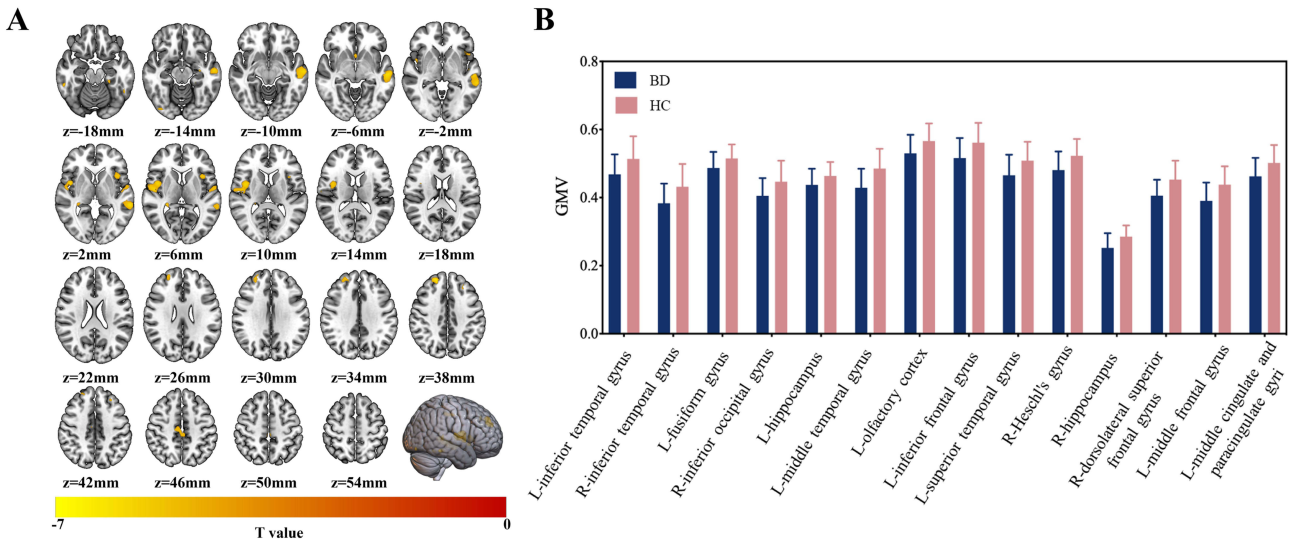

Figure 2 (**A** and **B**), respectively, shows the abnormal brain regions maps and differential changes between bipolar disorder (BD) and healthy controls (HC) in the grey matter volume (GMV) using the voxel-based morphometry (VBM) method.

The Correlations Between Brain Imaging Indicators and Clinical Variables in BD Patients

The comparison of DBM-GM, GMV, and WMV between BD patients and HC showed that the abnormal brain areas were not significantly correlated with the duration of illness and age of onset.

MVPA

The MVPA results are shown in Figures 5 and 6. The specific information on the performance of the classification model for distinguishing BD patients from HC were as follows in the GM region: (1) DBM-GM: The highest classification accuracy of 69.34% was achieved using 30% of features, along with an AUC of 0.72, sensitivity of 67.14%, specificity of 71.43%; (2) GMV: The highest classification accuracy of 72.42% was attained using 30% of features, along with an AUC of 0.78, sensitivity of 70.48%, and specificity of 74.29%; (3) GM Fusion (GMV and DBM-GM): Fusion led to a further improved highest classification accuracy of 73.72%, with an AUC of 0.73, sensitivity of 61.19%, and specificity of 85.71%. Permutation tests confirmed that abovementioned classification accuracies were significantly higher than random level ($P < 0.005$). Furthermore in the WM region, the performance of the classification model for distinguishing BD patients from HC showed

Table 2 The Abnormal Brain Regions of WMV in Bipolar Disorder Patients and Healthy Controls

Regions (AAL)	MNI			Number of Voxels	T value	Effect Size
	x	y	z			
R anterior cingulum	12	24	−3	201	−5.5041	−0.4196
L thalamus	−18	−18	6	431	−6.3138	−0.5822
R thalamus	16.5	−27	13.5	372	−5.9450	−0.5761
R inferior frontal gyrus	25.5	34.5	−6	21	−4.8786	−0.3367
R pallidum	16.5	1.5	1.5	33	−4.8025	−0.5383

Notes: T value: the statistic value at the peak voxel within clusters showing significant differences between bipolar disorder patients and healthy controls in the two-sample *t*-test with FWE voxel-level correction.
Abbreviations: WMV, white matter volume; AAL, anatomical automatic labeling; MNI, Montreal Neurological Coordinate; L, left; R, right.

https://doi.org/10.2147/NDT.S532650

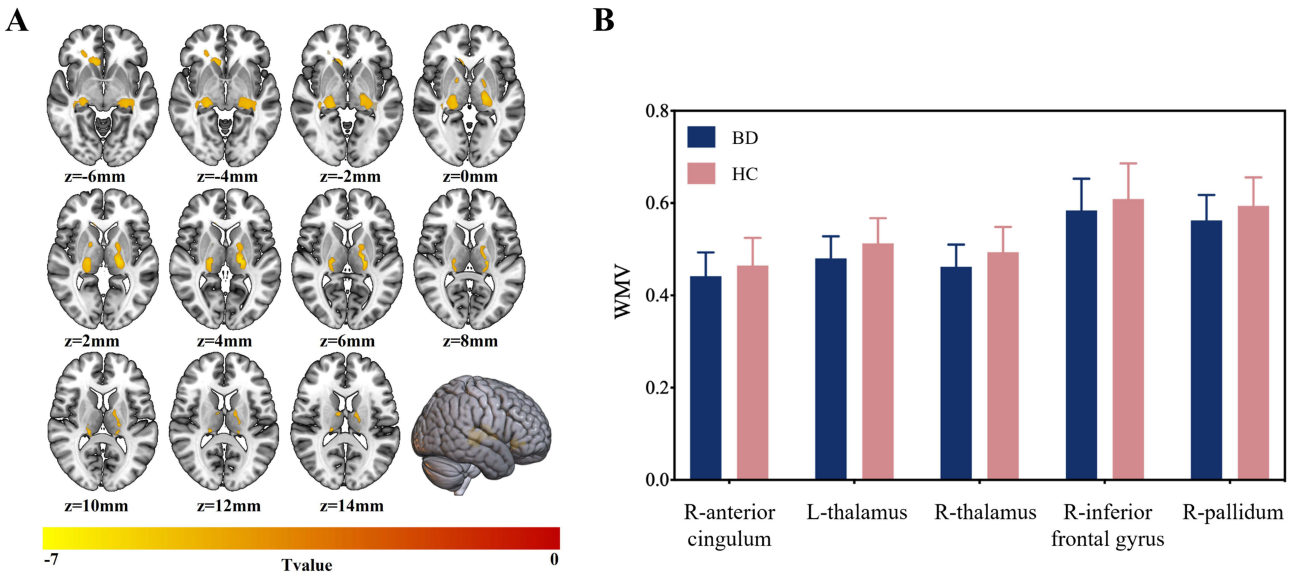

Figure 3 (**A** and **B**), respectively, shows the abnormal brain regions maps and differential changes between bipolar disorder (BD) and healthy controls (HC) in the white matter volume (WMV) using the voxel-based morphometry (VBM) method.

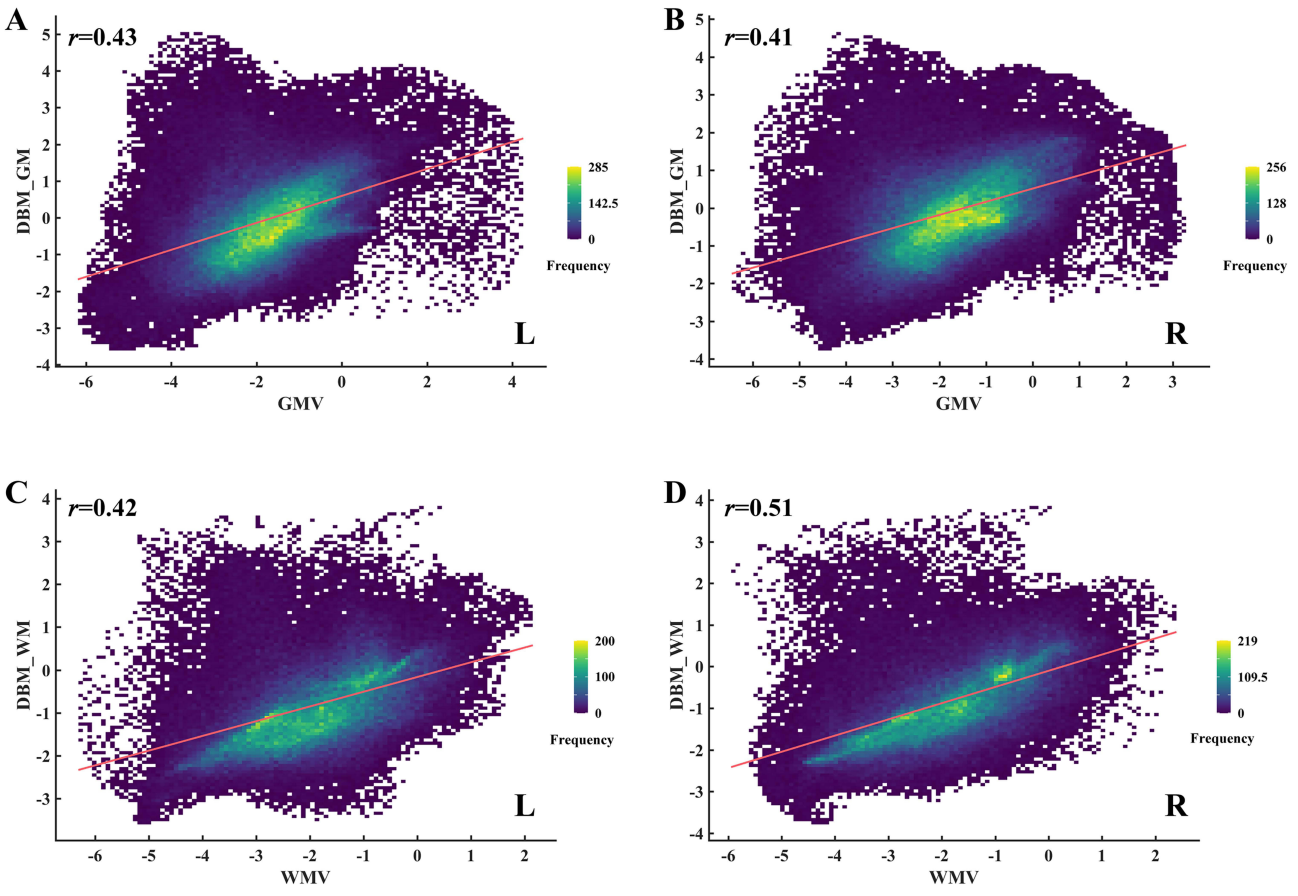

Figure 4 The spatial correlations of statistical maps generated by two brain structure imaging methods, with the Spearman correlation coefficient (r) presented on the top-left corner of each picture. (**A** and **B**) showed the spatial correlations between grey matter results detected by deformation-based morphometry (DBM-GM) and grey matter volume (GMV) in the left (L) and right (R) hemispheres, respectively; (**C** and **D**) showed the spatial correlations between white matter results detected by deformation-based morphometry (DBM-WM) and white matter volume (WMV) in the left (L) and right (R) hemispheres, respectively.

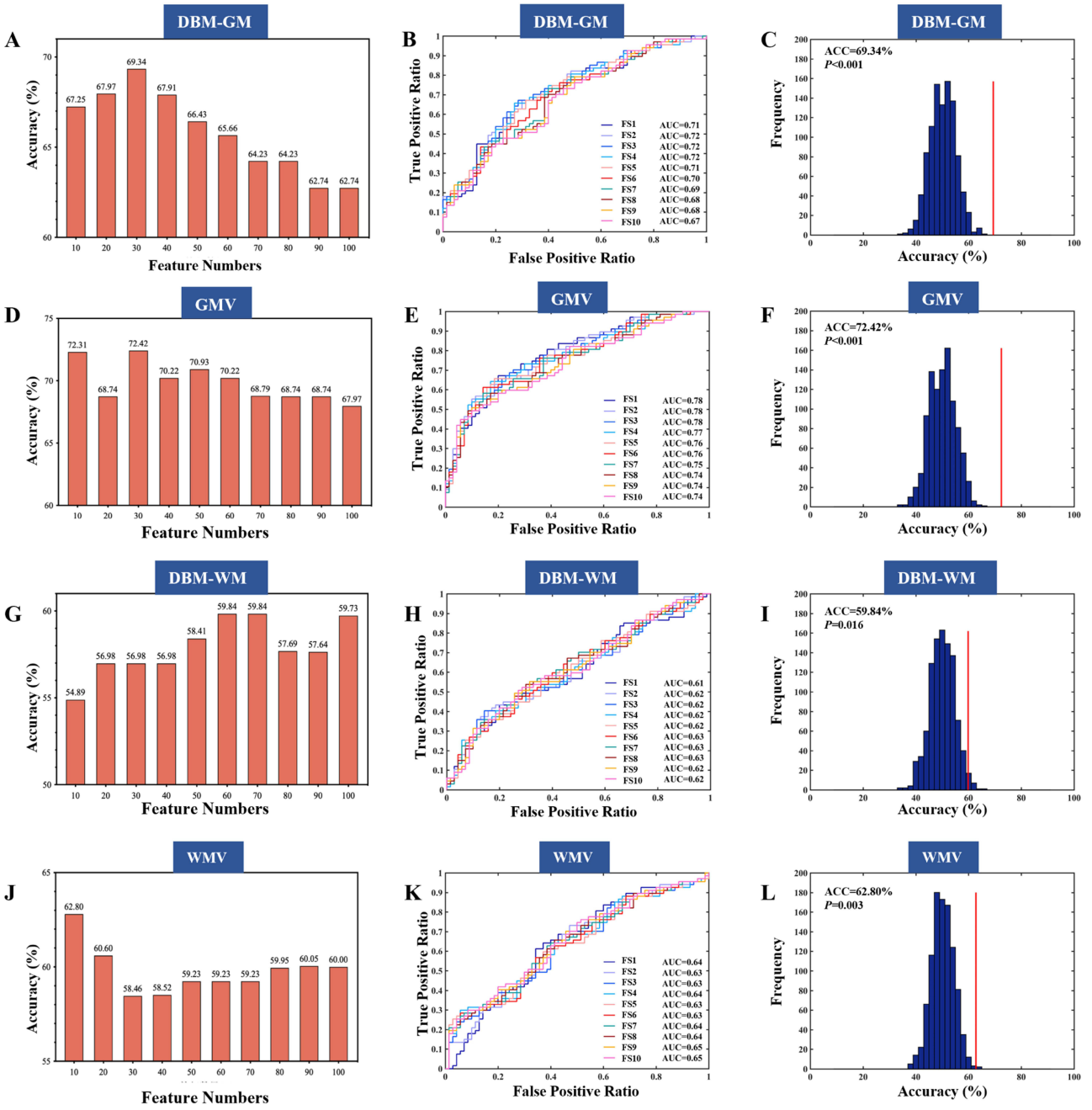

Figure 5 The multivariate pattern analysis (MVPA) results of grey matter results detected by deformation-based morphometry (DBM-GM), grey matter volume (GMV), white matter results detected by deformation-based morphometry (DBM-WM), and white matter volume (WMV) utilizing feature selection. (**A**–**C**) Results by the DBM-GM; (**D**–**F**) Results by the GMV; (**G**–**I**) Results by the DBM-WM, and (**J**–**L**) Results by the WMV. Within each row: The left column showed the feature numbers and accuracy (ACC); the middle column indicated the receiver operating characteristic (ROC) curve and area under the curve (AUCs) for each classifier when utilizing the feature selection; while the right column showed the highest classification ACC (the red vertical lines) and the zero distribution plots (blue color) of random classification ACC obtained after 1000 permutation tests when using feature selection.

the results below: (1) DBM-WM: The highest classification accuracy of 59.84% occurred when utilizing 70% of features, with corresponding AUC of 0.63, sensitivity of 60.95%, and specificity of 58.57%; (2) WMV: The highest classification accuracy of 62.80% was observed using 10% of features, resulting in an AUC of 0.64, sensitivity of 62.86%, and specificity of 62.86%; (3) WM Fusion (WMV and DBM-WM): The fusion model achieved a highest classification accuracy of 62.77%, with an AUC of 0.62, sensitivity of 46.27%, and specificity of 78.57%. Permutation tests confirmed that the classification accuracies of WMV and WM Fusion were significantly higher than random level ($P < 0.005$).

https://doi.org/10.2147/NDT.S532650

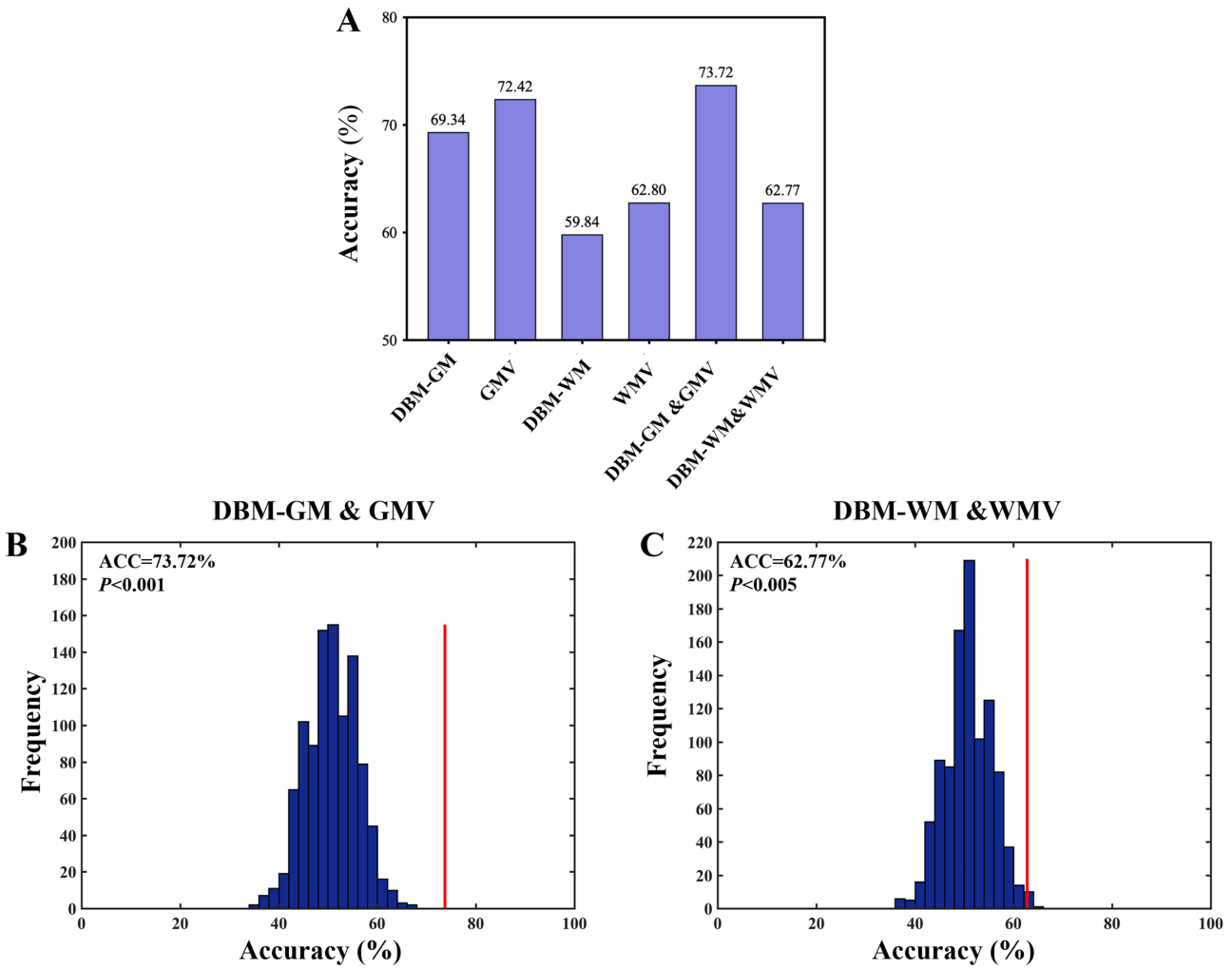

Figure 6 (**A**) The highest accuracy (ACC) of grey matter results detected by deformation-based morphometry (DBM-GM), grey matter volume (GMV), white matter results detected by deformation-based morphometry (DBM-WM), white matter volume (WMV), the fusion of DBM-GM and GMV, and the fusion of DBM-WM and WMV. (**B** and **C**) The highest classification ACC (red vertical lines) and the zero distribution plots (blue color) of random classification ACC obtained after 1000 permutation tests after fusion.

Discussion

Abnormal GM Structure in BD Patients

The GM area of the pregenual anterior cingulate cortex was increased in BD patients as indicated by DBM, which correlates with cognitive and emotional regulation, attention, problem-solving, motivation, and decision-making, functioning as a critical center for integrating cognitive and affective neuronal connections.[26] The anterior cingulate cortex can be divided into two subregions: pregenual anterior cingulate cortex and subgenual anterior cingulate cortex.[27,28] The pregenual anterior cingulate cortex is a component of the limbic system and the default mode network of the brain and establishes extensive connections with cortical and subcortical brain regions involved in emotional regulation and cognitive control.[29–32] Studies have identified that GM occupies the largest amount of neurons within the brain, and N-acetylasparte (NAA) exists in brain neurons and could be utilized as a marker to reflect neuron density.[33,34] Studies have reported that BD patients have increased NAA in the anterior cingulate gyrus.[35] Therefore, the above-mentioned backgrounds and the current research indicated that the neuron density within the pregenual anterior cingulate cortex could be increased in BD patients. The abnormal changes within such brain regions could potentially be a pathophysiological mechanism of BD patients. To date, there have been few studies related to the pregenual anterior cingulate cortex, of which the current study bridged the research gap. Additionally, the DBM study from our paper showed an increased left insula volume in the GM area in BD patients, which is a critical

component of the limbic system and is responsible for emotional regulation.[36,37] Similarly, one study using Positron Emission Computed Tomography (PET) imaging indicated an increased serotonin transporter binding-potential in the insula of BD patients.[38] Xu et al showed that the low-frequency amplitude of the insula was increased in BD patients.[39] Another study reported an overactivation of the insula region in BD patients upon the task related to emotional stimulations.[40] One investigation on the GM region of the insula showed that the GMV in the left dorsal anterior insula was increased in BD patients,[41] while another study found that the left insula GM density was increased in 11 BD patients.[42] The above-mentioned studies indicate the structural or functional changes in the insula region in BD patients. However, our study provided new evidence beyond such abnormal structure changes in the GM region of the insula. As the insula contains different regions, further studies could be performed more precisely on specific subregions within the insula to enhance the understanding of their functions.

This study found that GMV was decreased in numerous brain regions in VBM, including the temporal lobe, frontal lobe, occipital lobe, fusiform gyrus, hippocampus, olfactory cortex, and middle cingulate and paracingulate gyri (Table 1). However, no region showed an increase in GMV. The temporal lobe has been regarded with several functions, such as language comprehension, memory, and mental activity,[43] also the temporal lobe is connected to the prefrontal lobe and the limbic system via numerous neural connections and participates in the emotion-regulating processes.[44] Dysfunction of the frontotemporal neural network influenced emotional processing and regulation, which was considered the main cause of behavioral abnormalities in BD.[45] To date, numerous studies reported the cortical GM was thinned, and the GMV was decreased in the temporal and frontal regions in BD patients,[46–50] consisting with the results from the current study. The middle cingulate gyrus plays an important role in decision-making, especially in rewards-related decisions.[51] Previous studies suggested BD patients had cognition impairments,[52–54] and Neves Mde et al reported that the facial emotional cognitive score was positively correlated with the GMV of the middle cingulate gyrus in BD type I patients.[55] Another study showed that the middle cingulate gyrus was activated under negative emotional stimuli.[56] This study found a decrease in GMV of the middle cingulate gyrus in BD patients in VBM, suggesting that the atrophy of the middle cingulate gyrus in BD patients may be related to emotional cognitive impairment. The occipital lobe is the visual cortex center that mainly involved in the procession of visual information. Previous studies showed abnormal changes in visual functions from BD patients, which were related to visual perception disorders.[57,58] A study using 31P magnetic resonance spectroscopy (MRS) found that the ratio of phosphocreatine and adenosine triphosphate was changed in BD patients during occipital visual stimulation.[59] Moreover, Singh et al indicated that GMV was decreased in the inferior occipital gyrus and middle occipital gyrus in BD adolescences via a source-based morphometry method;[10] another large-scale MRI study showed a decreased occipital cortex thickness in BD patients, of which the reduction was positively correlated with the duration of illness.[46] The above-mentioned researches indicated that the occipital lobe brain region abnormalities could potentially be a pathophysiological mechanism of BD patients, which was reinforced by our study. It has been indicated that the fusiform gyrus was critical in visual perception, such as understanding and identifying color, in coordination with the occipital lobe. Besides, the fusiform gyrus is also closely related to the network that suppresses emotions,[60,61] which plays a key role in regulating emotions and impulses. Functional impairment of the fusiform gyrus was previously observed in BD patients.[60] Perlman et al found that adolescent BD patients showed a weakened activation of the left fusiform gyrus under the negative emotional face recognition tasks.[62] Another study found that BD patients have decreased GM density in the fusiform gyrus.[63] Our study also found that the GMV of the left fusiform gyrus was decreased from BD patients, suggesting that the abnormal GMV of the fusiform gyrus was closely related to negative emotions. Previous studies indicated that the cognitive domain that was severely impaired in BD patients was related with declarative memory.[64–66] Since hippocampus is an important structure for the acquisition, consolidation, and retrieval of declarative memory,[67] studies have reported a decrease in GMV[68–70] and neuron density[71–73] in the hippocampus of BD patients, which was consistent with our results. In addition, our study found that GMV in the olfactory cortex was decreased in BD patients. The olfactory cortex is located in the medial temporal lobe, containing the entorhinal and perirhinal cortex. The entorhinal cortex is closely related to the hippocampus, which delivers information into the hippocampal region and simultaneously transmits the information out of the hippocampal region to the cerebral cortex. As we can understand, there are still no relevant studies on the structure and function of the olfactory cortex in BD patients. Previous studies have shown that the entorhinal cortex is closely related to cognitive function. A meta-analysis reported the occurrence of brain atrophy in mild cognitive impairment patients, within which the most influenced regions were the entorhinal cortex and

hippocampus;[74] another study suggested that the decrease in the volume of the entorhinal cortex was associated with a decrease in declarative memory scores.[75] In conclusion, our study indicated that a declarative memory deficit in BD may be related to GMV atrophy in the hippocampus and olfactory cortex brain regions. Besides, we further measured the spatial correlation between GMV and DBM-GM statistical maps, and the results showed that the two indicators were moderately correlated in the left and right hemispheres, suggesting that both indicators could reflect brain structural changes with consistent trends in certain brain regions. However, we observed that the two indicators yielded different results in the inter-group correlation analysis, which could be attributed to two reasons: One was the different threshold of statistical significance from each indicator; the other was the similarity and specificity of the two indicators in measuring the brain structural information, which were extracted by different methods from different aspects. Hence, these indicators might have varied sensitivity in investigating different types of brain structural changes.

Abnormal WM Structure in BD Patients

The WM region mainly belongs to the area where nerve fibers gather, which is composed of neurites surrounded by myelin sheaths in neurons, responsible for transmitting information within the brain. The WM could ensure the efficiency and accuracy of neural information transmission. Meanwhile, it is also involved in emotional regulation and maintains cognitive function. Numerous studies have suggested that abnormalities in WM play an important role in the pathophysiological mechanism of BD.[76–79] It was previously recognized by the neuroanatomical circuit theory that the "limbic-thalamic-cortical" and "limbic-cortical-striatal-pallidal-thalamic" circuits play a key role in executive function and emotion regulation.[80] The limbic-striatal-pallidal-thalamic is currently the main neural circuit that elucidates the pathophysiological mechanism of affective disorders.[81] The prefrontal lobe is an important hub in two neuroanatomical circuits. In the above-mentioned circuits, our study indicated that WMV was decreased in the bilateral thalamus, right inferior frontal gyrus, pallidum, and anterior cingulate gyrus in BD patients, showing abnormal changes in the structure of WM in these brain regions (Table 2). The prefrontal lobe is an important brain region that regulates emotion and executive function and is related to emotion, cognition, language function, and behavior control,[82,83] the damage and dysfunction of which were closely related to emotional regulation disorders.[80,84,85] Some studies have shown that changes in WM integrity in BD patients were mainly presented in the frontal lobe region.[86,87] Several studies revealed a T2 or FLAIR hyper-intensity in the deep prefrontal lobe and periventricular WM.[88,89] Haznedar et al found that the WMV in the frontal cortex was significantly reduced in patients with bipolar spectrum disorders.[90] In the study of MRS in BD patients, a decrease in neuronal density in the prefrontal WM region was revealed.[91,92] The anterior cingulum is the main WM region that connects the limbic system to the frontal lobe region.[93,94] Previous studies on brain function and structure suggested abnormalities in the anterior cingulum, which was related to the pathogenesis of BD.[95] A meta-analysis study on diffusion tensor imaging showed the fractional anisotropy (FA) of WM was decreased in the adjacent right anterior and subgenual cingulate cortex in BD patients.[96] Gao et al reported a significantly reduced FA value in the right anterior cingulate in their study regarding manic episodes in BD adolescents.[97] Another study divided the cingulum into anterior and posterior cingulum and compared the difference of FA values in both areas between the BD patients and the HC groups. The results showed that the FA values were decreased in both anterior and posterior cingulum in BD patients. However, the changes in posterior cingulum were not significant.[94] The thalamus is a relay station that connects the cortex with both the subcortical structures and different cortical regions. It has been reported that the thalamus is functionally involved in regulating emotion, cognition, and social behavior.[98] Ishida et al reported that BD patients (n = 29) had significantly decreased local WMV values as compared with HC controls (n = 33) in the bilateral posterior thalami.[99] Another study in BD patients similarly found a decreased WMV in the right thalamus.[100] The pallidum is an important part of the basal ganglia located deep in both cerebral hemispheres. The involvement of WM in the basal ganglia may be related to affective disorders, as reported by several studies,[101,102] and the pallidotomy could potentially induce a transient manic state.[103] The above-mentioned research suggested abnormal structural changes could potentially occur in the WMV of pallidum from BD patients. There have been few studies on WMV in BD patients with inconsistent conclusions. Therefore, the current study provided a new vision that the WMV abnormality in multiple brain regions could potentially be presented in the limbic-striatal-pallidal-thalamic neural circuit of BD patients. In addition, our study did not detect significant differences in the WM regions between the BD patients' group and the HC group in DBM.

However, in spatial correlation analysis, the results of our study showed a moderate correlation between WMV and DBM-WM in both left and right cerebral hemispheres, suggesting that there was also the abnormity of WM structure in some brain regions in DBM in BD patients, but with low statistical significance. Further studies could expand the sample sizes to better explore the pathophysiological mechanism of the structural changes of WM region in BD patients in DBM.

MVPA

To date, there are still many challenges in the diagnosis of BD. The current diagnosis of BD is mainly based on the DSM, International Classification of Diseases (ICD), and combined with psychological examination scales for clinical evaluation. It is usually diagnosed based on clinical observation and checks, the behavioral symptoms of patients, and the descriptions from patients and guardians, which are subjective and could compromise the accuracy of diagnosis.[104,105] In recent years, with the continuous development of artificial intelligence technology, many studies have attempted to use neuroimaging indicators to develop a more objective tool that can be used in the auxiliary diagnosis of BD. Deng et al found that the FA value of the left anterior thalamic radiation could be used to distinguish BD from major depressive disorder using the SVM classification algorithm, with a classification accuracy of 68.33%.[106] Another study used VBM to classify BD patients and HC, with an accuracy rate of 58.3%.[23] However, most of the related studies focus on a single imaging indicator, and the classification accuracy of different structural imaging indicators obtained from different studies is not comparable. In this study, we used the same classification algorithm in the same group of subjects to examine the classification and diagnostic abilities of DBM and VBM indicators for BD patients and HC, and the specific results were as follows: in the GM region, based on SVM classification algorithm, the highest classification accuracy of GMV indicator in distinguishing BD patients from HC was 72.42%, and the highest classification accuracy of DBM-GM was 69.34%, suggesting that both GMV and DBM-GM indicators have good recognition ability in the diagnosis of BD patients at the individual level. In addition, the highest classification accuracy was 73.72%, obtained by fusing the GMV and DBM-GM indicators, significantly higher than the highest classification accuracy achieved by using any single indicator, showing that DBM-GM and GMV generated different information that could mutually complement in depicting the abnormal brain changes of BD patients. A study in patients with first-episode schizophrenia also found that the classification accuracy of combining VBM and DBM was 5% higher than those utilizing VBM or DBM alone.[24] In the future, we should consider combining different structural imaging indicators when developing neuroimage-assisted diagnostic tools for BD. In addition to the GM region, we also analyzed the WM region, and the results showed that the highest classification accuracy of using the WMV indicator based on the SVM classification algorithm to distinguish BD patients from HC was 62.80%, suggesting that WMV could distinguish the BD patients from HC more accurately. However, the highest classification accuracy of DBM-WM in distinguishing BD patients from HC was 59.84%, which was lower than the classification accuracy at the random level, suggesting that the WM may not be as effective as GM in recognizing BD from HC. Besides, fusing DBM-WM and WMV indicators showed no improvements in the highest classification accuracy (62.77%), indicating that in the WM region, DBM-WM may not provide additional complementary information, and most of the information that could be utilized in the classification model may still be based on the WMV results. Considering that the current study is pioneering in utilizing VBM and DBM in WM, further exploration could be performed to reinforce or validate the results. In conclusion, our study indicates that the use of DBM and VBM methods can discover potential neuroimaging biomarkers in BD patients, and the combination of the two indicators can be used as a neuroimaging auxiliary for diagnosing BD in the future.

To the best of our knowledge, there were still no studies that utilized the DBM method to explore the morphological changes of GM and WM regions in BD patients, of which the current study bridged the research gap. Moreover, we also compared the results by DBM and conventional VBM methods, in terms of the GM and WM regions in BD patients, which facilitated a new insight in deciphering the pathophysiological changes of BD. The same algorithm was utilized to investigate the indicator of DBM-GM, GMV, DBM-WM, WMV, and fusion of DBM-GM with GMV, fusion of DBM-WM with WMV, by their capacity to diagnose and recognize BD patients.

We also acknowledged several limitations in the current study that could be improved in future studies. First, this study was cross-sectional with a limited sample size, all participants were recruited from the single center. This limits the in-depth analysis of different clinical subtypes of BD, and the model could still be improved in various diagnostic performance indicators, such as sensitivity, specificity, and AUC. In the future, we will integrate multicenter large sample clinical data and

perform long-term longitudinal follow-up studies to explore the changes in brain structure of BD patients with different clinical types, and further improve the generalization ability of the model. Second, the current study only focused on analyzing the fusion of two structural imaging indicators, but did not include functional modal data. Meanwhile, the leave-one-out cross-validation (LOOCV) method was not adopted in this study.[107] Future studies will integrate functional imaging data and, when computational resources permit, employ methods such as LOOCV to further explore the classification efficacy of multimodal imaging indicators and the robustness of validation results. Finally, this study did not include major depressive disorder (MDD) as the control group, and therefore cannot evaluate the specificity of brain imaging indicators in distinguishing BD and MDD. In clinical practices, the diagnosis of mental disorders mainly based on the clinical diagnostic criteria, and the subthreshold affective states of MDD patients could be underestimated in clinical records, resulting in biased diagnosis of patients. Therefore, for future researches, we will expand the patients recruitment to both increase sample size and include MDD patients, to clarify the practical value of brain imaging indicators in distinguishing BD from MDD.

Conclusions

The DBM method within the current study revealed that the volume of the insula and pregenual anterior cingulate cortex were increased in BD patients in the GM area. Moreover, the VBM method indicated found that the GMV from the inferior temporal gyrus, hippocampus, inferior frontal gyrus, olfactory cortex, fusiform gyrus, middle temporal gyrus, superior temporal gyrus, middle frontal gyrus, middle cingulate and paracingulate gyri, inferior occipital gyrus, Heschl's gyrus, and dorsolateral superior frontal gyrus were decreased. Similarly, the WMV from the thalamus, inferior frontal gyrus, pallidum, and anterior cingulum were decreased in BD patients. In addition, MVPA showed that all three structural imaging indicators, namely DBM-GM, GMV, and WMV showed their capabilities in diagnosing on the individual level of BD patients, and fusing the two structural imaging indicators of DBM-GM and GMV in the GM area could significantly improve the classification accuracy, providing a new insight for developing auxiliary diagnostic tools towards BD via artificial intelligence in the future.

Data Sharing Statement

The original contributions presented in the study are included in the article, further inquiries can be directed to the corresponding authors.

Ethics Approval and Informed Consent

This study was approved by the Ethics Committee of Tianjin Fourth Central Hospital (Ethics Approval No. SZXLL-2021-KY031). All subjects knew about this study and signed informed consent. All procedures carried out in studies conformed to the 1964 Helsinki Declaration and its subsequent amendments or similar ethical standards.

Acknowledgments

We are grateful to all the participants involved in this study.

Author Contributions

All authors made a significant contribution to the work reported, whether that is in the conception, study design, execution, acquisition of data, analysis and interpretation, or in all these areas; took part in drafting, revising or critically reviewing the article; gave final approval of the version to be published; have agreed on the journal to which the article has been submitted; and agree to be accountable for all aspects of the work.

Funding

This work was supported by grants from the National Natural Science Foundation of China (Grant Nos. 81761128032 and 82471554), Clinical Research Plan of SHDC (Grant No. SHDC12020126), Key Area Research and Development Program of Guangdong Province (Grant No. 2018B030334001), Clinical Research Center of Shanghai Mental Health Center Key Project (Grant No. CRC2021ZD01), China Postdoctoral Science Foundation (2024M761870), and Sailing Plan Talent Project of Shanghai Mental Health Center (Grant No. 2024-QH-05).

Disclosure

The authors report no conflicts of interest in this work.

References

1. Alonso J, Petukhova M, Vilagut G, et al. Days out of role due to common physical and mental conditions: results from the WHO World Mental Health surveys. *Mol Psychiatry*. 2011;16(12):1234–1246. doi:10.1038/mp.2010.101
2. Simon GE. Social and economic burden of mood disorders. *Biol Psychiatry*. 2003;54(3):208–215. doi:10.1016/s0006-3223(03)00420-7
3. Pompili M, Gonda X, Serafini G, et al. Epidemiology of suicide in bipolar disorders: a systematic review of the literature. *Bipolar Disord*. 2013;15(5):457–490. doi:10.1111/bdi.12087
4. Plans L, Barrot C, Nieto E, et al. Association between completed suicide and bipolar disorder: a systematic review of the literature. *J Affect Disord*. 2019;242:111–122. doi:10.1016/j.jad.2018.08.054
5. Malhi GS, Outhred T, Das P, et al. Modeling suicide in bipolar disorders. *Bipolar Disord*. 2018;20(4):334–348. doi:10.1111/bdi.12622
6. Hansson C, Joas E, Pålsson E, et al. Risk factors for suicide in bipolar disorder: a cohort study of 12850 patients. *Acta Psychiatr Scand*. 2018;138(5):456–463. doi:10.1111/acps.12946
7. Ayık B, Baş A, Usta Sağlam NG, Izci F. The relationship between emotional dysregulation, alexithymia and somatization in patients with bipolar disorder. *Alpha Psychiatry*. 2023;24(1):15–21. doi:10.5152/alphapsychiatry.2023.22974
8. Aguglia A, Giacomini G, De Michiel CF, et al. Characterization of bipolar disorder i and ii: clinical features, comorbidities, and pharmacological pattern. *Alpha Psychiatry*. 2024;25(4):472–479. doi:10.5152/alphapsychiatry.2024.241474
9. Scanlon C, Mueller SG, Tosun D, et al. Impact of methodologic choice for automatic detection of different aspects of brain atrophy by using temporal lobe epilepsy as a model. *AJNR Am J Neuroradiol*. 2011;32(9):1669–1676. doi:10.3174/ajnr.A2578
10. Singh A, Arya A, Agarwal V, Shree R, Kumar U. Grey and white matter alteration in euthymic children with bipolar disorder: a combined source-based morphometry (SBM) and voxel-based morphometry (VBM) study. *Brain Imaging Behav*. 2022;16(1):22–30. doi:10.1007/s11682-021-00473-0
11. Madeira N, Duarte JV, Martins R, et al. Morphometry and gyrification in bipolar disorder and schizophrenia: a comparative MRI study. *Neuroimage Clin*. 2020;26:102220. doi:10.1016/j.nicl.2020.102220
12. Lee DK, Lee H, Park K, et al. Common gray and white matter abnormalities in schizophrenia and bipolar disorder. *PLoS One*. 2020;15(5):e0232826. doi:10.1371/journal.pone.0232826
13. Volz H, Gaser C, Sauer H. Supporting evidence for the model of cognitive dysmetria in schizophrenia--a structural magnetic resonance imaging study using deformation-based morphometry. *Schizophr Res*. 2000;46(1):45–56. doi:10.1016/s0920-9964(99)00236-4
14. Xiaodan L, Meng L, Lingsheng L, Zepu R, Ping M. A deformation-based morphometry study on gray matter abnormalities in drug-naive patients with first-onset major depressive disorder. *Chin J Psych*. 2021;2021(2):104–110.
15. Nielsen AN, Barch DM, Petersen SE, Schlaggar BL, Greene DJ. Machine learning with neuroimaging: evaluating its applications in psychiatry. *Biol Psychiatry Cogn Neurosci Neuroimaging*. 2020;5(8):791–798. doi:10.1016/j.bpsc.2019.11.007
16. Orban P, Dansereau C, Desbois L, et al. Multisite generalizability of schizophrenia diagnosis classification based on functional brain connectivity. *Schizophr Res*. 2018;192:167–171. doi:10.1016/j.schres.2017.05.027
17. Librenza-Garcia D, Kotzian BJ, Yang J, et al. The impact of machine learning techniques in the study of bipolar disorder: a systematic review. *Neurosci Biobehav Rev*. 2017;80:538–554. doi:10.1016/j.neubiorev.2017.07.004
18. Schwarz E, Doan NT, Pergola G, et al. Reproducible grey matter patterns index a multivariate, global alteration of brain structure in schizophrenia and bipolar disorder. *Transl Psychiatry*. 2019;9(1):12. doi:10.1038/s41398-018-0225-4
19. Yang J, Pu W, Ouyang X, et al. Abnormal connectivity within anterior cortical midline structures in bipolar disorder: evidence from integrated MRI and functional MRI. *Front Psychiatry*. 2019;10:788. doi:10.3389/fpsyt.2019.00788
20. Ji L, Meda SA, Tamminga CA, et al. Characterizing functional regional homogeneity (ReHo) as a B-SNIP psychosis biomarker using traditional and machine learning approaches. *Schizophr Res*. 2020;215:430–438. doi:10.1016/j.schres.2019.07.015
21. Li H, Cui L, Cao L, et al. Identification of bipolar disorder using a combination of multimodality magnetic resonance imaging and machine learning techniques. *BMC Psychiatry*. 2020;20(1):488. doi:10.1186/s12888-020-02886-5
22. Salvador R, Radua J, Canales-Rodríguez EJ, et al. Evaluation of machine learning algorithms and structural features for optimal MRI-based diagnostic prediction in psychosis. *PLoS One*. 2017;12(4):e0175683. doi:10.1371/journal.pone.0175683
23. Matsuo K, Harada K, Fujita Y, et al. Distinctive neuroanatomical substrates for depression in bipolar disorder versus major depressive disorder. *Cereb Cortex*. 2019;29(1):202–214. doi:10.1093/cercor/bhx319
24. Ediri Arachchi W, Peng Y, Zhang X, et al. A systematic characterization of structural brain changes in schizophrenia. *Neurosci Bull*. 2020;36(10):1107–1122. doi:10.1007/s12264-020-00520-8
25. Peng Y, Zhang X, Li Y, et al. MVPANI: a toolkit with friendly graphical user interface for multivariate pattern analysis of neuroimaging data. *Front Neurosci*. 2020;14:545. doi:10.3389/fnins.2020.00545
26. Kandilarova S, Stoyanov D, Sirakov N, Maes M, Specht K. Reduced grey matter volume in frontal and temporal areas in depression: contributions from voxel-based morphometry study. *Acta Neuropsychiatr*. 2019;31(5):252–257. doi:10.1017/neu.2019.20
27. Rolls ET, Huang CC, Lin CP, Feng J, Joliot M. Automated anatomical labelling atlas 3. *Neuroimage*. 2020;206:116189. doi:10.1016/j.neuroimage.2019.116189
28. Du J, Rolls ET, Cheng W, et al. Functional connectivity of the orbitofrontal cortex, anterior cingulate cortex, and inferior frontal gyrus in humans. *Cortex*. 2020;123:185–199. doi:10.1016/j.cortex.2019.10.012
29. Keramatian K, Chakrabarty T, Saraf G, Pinto JV, Yatham LN. Grey matter abnormalities in first-episode mania: a systematic review and meta-analysis of voxel-based morphometry studies. *Bipolar Disord*. 2021;23(3):228–240. doi:10.1111/bdi.12995
30. Palomero-Gallagher N, Hoffstaedter F, Mohlberg H, et al. Human pregenual anterior cingulate cortex: structural, functional, and connectional heterogeneity. *Cereb Cortex*. 2019;29(6):2552–2574. doi:10.1093/cercor/bhy124

31. Allman JM, Hakeem A, Erwin JM, Nimchinsky E, Hof P. The anterior cingulate cortex. The evolution of an interface between emotion and cognition. *Ann N Y Acad Sci*. 2001;935:107–117. doi:10.1111/j.1749-6632.2001.tb03476.x
32. Rolls ET. The cingulate cortex and limbic systems for emotion, action, and memory. *Brain Struct Funct*. 2019;224(9):3001–3018. doi:10.1007/s00429-019-01945-2
33. Simmons ML, Frondoza CG, Coyle JT. Immunocytochemical localization of N-acetyl-aspartate with monoclonal antibodies. *Neuroscience*. 1991;45(1):37–45. doi:10.1016/0306-4522(91)90101-s
34. Baslow MH. N-acetylaspartate in the vertebrate brain: metabolism and function. *Neurochem Res*. 2003;28(6):941–953. doi:10.1023/a:1023250721185
35. Soeiro-de-souza MG, Otaduy MCG, Machado-Vieira R, et al. Lithium-associated anterior cingulate neurometabolic profile in euthymic Bipolar I disorder: A ^{1}H-MRS study. *J Affect Disord*. 2018;241:192–199. doi:10.1016/j.jad.2018.08.039
36. Cui L, Li H, Li JB, et al. Altered cerebellar gray matter and cerebellar-cortex resting-state functional connectivity in patients with bipolar disorder I. *J Affect Disord*. 2022;302:50–57. doi:10.1016/j.jad.2022.01.073
37. Phan KL, Wager T, Taylor SF, Liberzon I. Functional neuroanatomy of emotion: a meta-analysis of emotion activation studies in PET and fMRI. *Neuroimage*. 2002;16(2):331–348. doi:10.1006/nimg.2002.1087
38. Cannon DM, Ichise M, Rollis D, et al. Elevated serotonin transporter binding in major depressive disorder assessed using positron emission tomography and [11C]DASB; comparison with bipolar disorder. *Biol Psychiatry*. 2007;62(8):870–877. doi:10.1016/j.biopsych.2007.03.016
39. Xu K, Liu H, Li H, et al. Amplitude of low-frequency fluctuations in bipolar disorder: a resting state fMRI study. *J Affect Disord*. 2014;152-154:237–242. doi:10.1016/j.jad.2013.09.017
40. Chan CC, Alter S, Hazlett EA, et al. Neural correlates of impulsivity in bipolar disorder: a systematic review and clinical implications. *Neurosci Biobehav Rev*. 2023;147:105109. doi:10.1016/j.neubiorev.2023.105109
41. Tang LR, Liu CH, Jing B, et al. Voxel-based morphometry study of the insular cortex in bipolar depression. *Psychiatry Res*. 2014;224(2):89–95. doi:10.1016/j.pscychresns.2014.08.004
42. Lochhead RA, Parsey RV, Oquendo MA, Mann JJ. Regional brain gray matter volume differences in patients with bipolar disorder as assessed by optimized voxel-based morphometry. *Biol Psychiatry*. 2004;55(12):1154–1162. doi:10.1016/j.biopsych.2004.02.026
43. Geng Y, Bi C, Zhang R. High risk factors and preventive measures of bipolar disorder after ischemic stroke. *Alpha Psychiatry*. 2024;25(2):220–225. doi:10.5152/alphapsychiatry.2024.231467
44. Mitchell RL, Elliott R, Barry M, Cruttenden A, Woodruff PW. The neural response to emotional prosody, as revealed by functional magnetic resonance imaging. *Neuropsychologia*. 2003;41(10):1410–1421. doi:10.1016/s0028-3932(03)00017-4
45. Phillips ML, Swartz HA. A critical appraisal of neuroimaging studies of bipolar disorder: toward a new conceptualization of underlying neural circuitry and a road map for future research. *Am J Psychiatry*. 2014;171(8):829–843. doi:10.1176/appi.ajp.2014.13081008
46. Hibar DP, Westlye LT, Doan NT, et al. Cortical abnormalities in bipolar disorder: an MRI analysis of 6503 individuals from the ENIGMA bipolar disorder working group. *Mol Psychiatry*. 2018;23(4):932–942. doi:10.1038/mp.2017.73
47. Okanda Nyatega C, Qiang L, Jajere Adamu M, Bello Kawuwa H. Altered striatal functional connectivity and structural dysconnectivity in individuals with bipolar disorder: a resting state magnetic resonance imaging study. *Front Psychiatry*. 2022;13:1054380. doi:10.3389/fpsyt.2022.1054380
48. Maggioni E, Crespo-Facorro B, Nenadic I, et al. Common and distinct structural features of schizophrenia and bipolar disorder: the European network on psychosis, affective disorders and cognitive trajectory (ENPACT) study. *PLoS One*. 2017;12(11):e0188000. doi:10.1371/journal.pone.0188000
49. Wang X, Tian F, Wang S, et al. Gray matter bases of psychotic features in adult bipolar disorder: a systematic review and voxel-based meta-analysis of neuroimaging studies. *Hum Brain Mapp*. 2018;39(12):4707–4723. doi:10.1002/hbm.24316
50. Lu X, Zhong Y, Ma Z, et al. Structural imaging biomarkers for bipolar disorder: Meta-analyses of whole-brain voxel-based morphometry studies. *Depress Anxiety*. 2019;36(4):353–364. doi:10.1002/da.22866
51. Van heukelum S, Mars RB, Guthrie M, et al. Where is cingulate cortex? A cross-species view. *Trends Neurosci*. 2020;43(5):285–299. doi:10.1016/j.tins.2020.03.007
52. Gillissie ES, Lui LMW, Ceban F, et al. Deficits of social cognition in bipolar disorder: systematic review and meta-analysis. *Bipolar Disord*. 2022;24(2):137–148. doi:10.1111/bdi.13163
53. Saldarini F, Gottlieb N, Stokes PRA. Neural correlates of working memory function in euthymic people with bipolar disorder compared to healthy controls: a systematic review and meta-analysis. *J Affect Disord*. 2022;297:610–622. doi:10.1016/j.jad.2021.10.084
54. Wang Y, Meng W, Liu Z, An Q, Hu X. Cognitive impairment in psychiatric diseases: biomarkers of diagnosis, treatment, and prevention. *Front Cell Neurosci*. 2022;16:1046692. doi:10.3389/fncel.2022.1046692
55. Neves Mde C, Albuquerque MR, Malloy-Diniz L, et al. A voxel-based morphometry study of gray matter correlates of facial emotion recognition in bipolar disorder. *Psychiatry Res*. 2015;233(2):158–164. doi:10.1016/j.pscychresns.2015.05.009
56. Seehausen M, Kazzer P, Bajbouj M, et al. Talking about social conflict in the MRI scanner: neural correlates of being empathized with. *Neuroimage*. 2014;84:951–961. doi:10.1016/j.neuroimage.2013.09.056
57. O'Bryan RA, Brenner CA, Hetrick WP, O'Donnell BF. Disturbances of visual motion perception in bipolar disorder. *Bipolar Disord*. 2014;16(4):354–365. doi:10.1111/bdi.12173
58. Chen Y, Levy DL, Sheremata S, Holzman PS. Bipolar and schizophrenic patients differ in patterns of visual motion discrimination. *Schizophr Res*. 2006;88(1–3):208–216. doi:10.1016/j.schres.2006.06.004
59. Yuksel C, Du F, Ravichandran C, et al. Abnormal high-energy phosphate molecule metabolism during regional brain activation in patients with bipolar disorder. *Mol Psychiatry*. 2015;20(9):1079–1084. doi:10.1038/mp.2015.13
60. Strakowski SM, Adler CM, Holland SK, Mills N, DelBello MP. A preliminary FMRI study of sustained attention in euthymic, unmedicated bipolar disorder. *Neuropsychopharmacology*. 2004;29(9):1734–1740. doi:10.1038/sj.npp.1300492
61. Yamasaki H, LaBar KS, McCarthy G. Dissociable prefrontal brain systems for attention and emotion. *Proc Natl Acad Sci U S A*. 2002;99(17):11447–11451. doi:10.1073/pnas.182176499
62. Perlman SB, Fournier JC, Bebko G, et al. Emotional face processing in pediatric bipolar disorder: evidence for functional impairments in the fusiform gyrus. *J Am Acad Child Adolesc Psychiatry*. 2013;52(12):1314–1325.e1313. doi:10.1016/j.jaac.2013.09.004

63. James A, Hough M, James S, et al. Structural brain and neuropsychometric changes associated with pediatric bipolar disorder with psychosis. *Bipolar Disord*. 2011;13(1):16–27. doi:10.1111/j.1399-5618.2011.00891.x
64. Altshuler LL, Ventura J, van Gorp WG, et al. Neurocognitive function in clinically stable men with bipolar I disorder or schizophrenia and normal control subjects. *Biol Psychiatry*. 2004;56(8):560–569. doi:10.1016/j.biopsych.2004.08.002
65. Bearden CE, Glahn DC, Monkul ES, et al. Sources of declarative memory impairment in bipolar disorder: mnemonic processes and clinical features. *J Psychiatr Res*. 2006;40(1):47–58. doi:10.1016/j.jpsychires.2005.08.006
66. Robinson LJ, Ferrier IN. Evolution of cognitive impairment in bipolar disorder: a systematic review of cross-sectional evidence. *Bipolar Disord*. 2006;8(2):103–116. doi:10.1111/j.1399-5618.2006.00277.x
67. Eichenbaum H. A cortical-hippocampal system for declarative memory. *Nat Rev Neurosci*. 2000;1(1):41–50. doi:10.1038/35036213
68. Xiao Q, Zhong Y, Jiao Q, Lu G, Su Y. Gray matter voxel-based morphometry in mania and remission states of children with bipolar disorder. *J Affect Disord*. 2020;268:47–54. doi:10.1016/j.jad.2020.02.042
69. Wise T, Radua J, Via E, et al. Common and distinct patterns of grey-matter volume alteration in major depression and bipolar disorder: evidence from voxel-based meta-analysis. *Mol Psychiatry*. 2017;22(10):1455–1463. doi:10.1038/mp.2016.72
70. Yang Y, Li X, Cui Y, et al. Reduced gray matter volume in orbitofrontal cortex across schizophrenia, major depressive disorder, and bipolar disorder: a comparative imaging study. *Front Neurosci*. 2022;16:919272. doi:10.3389/fnins.2022.919272
71. Capizzano AA, Jorge RE, Acion LC, Robinson RG. In vivo proton magnetic resonance spectroscopy in patients with mood disorders: a technically oriented review. *J Magn Reson Imaging*. 2007;26(6):1378–1389. doi:10.1002/jmri.21144
72. Deicken RF, Pegues MP, Anzalone S, Feiwell R, Soher B. Lower concentration of hippocampal N-acetylaspartate in familial bipolar I disorder. *Am J Psychiatry*. 2003;160(5):873–882. doi:10.1176/appi.ajp.160.5.873
73. Blasi G, Bertolino A, Brudaglio F, et al. Hippocampal neurochemical pathology in patients at first episode of affective psychosis: a proton magnetic resonance spectroscopic imaging study. *Psychiatry Res*. 2004;131(2):95–105. doi:10.1016/j.pscychresns.2003.11.002
74. Tabatabaei-Jafari H, Shaw ME, Cherbuin N. Cerebral atrophy in mild cognitive impairment: a systematic review with meta-analysis. *Alzheimers Dement*. 2015;1(4):487–504. doi:10.1016/j.dadm.2015.11.002
75. Stoub TR, Rogalski EJ, Leurgans S, Bennett DA, deToledo-Morrell L. Rate of entorhinal and hippocampal atrophy in incipient and mild AD: relation to memory function. *Neurobiol Aging*. 2010;31(7):1089–1098. doi:10.1016/j.neurobiolaging.2008.08.003
76. Delvecchio G, Pigoni A, Bauer IE, Soares JC, Brambilla P. Disease-discordant twin structural MRI studies on affective disorders. *Neurosci Biobehav Rev*. 2020;108:459–471. doi:10.1016/j.neubiorev.2019.11.023
77. Ho NF, Li hui chong P, Lee DR, et al. The amygdala in schizophrenia and bipolar disorder: a synthesis of structural MRI, diffusion tensor imaging, and resting-state functional connectivity findings. *Harv Rev Psychiatry*. 2019;27(3):150–164. doi:10.1097/hrp.0000000000000207
78. Poletti S, Melloni E, Aggio V, et al. Grey and white matter structure associates with the activation of the tryptophan to kynurenine pathway in bipolar disorder. *J Affect Disord*. 2019;259:404–412. doi:10.1016/j.jad.2019.08.034
79. Zhang R, Shao R, Xu G, et al. Aberrant brain structural-functional connectivity coupling in euthymic bipolar disorder. *Hum Brain Mapp*. 2019;40(12):3452–3463. doi:10.1002/hbm.24608
80. Price JL, Drevets WC. Neural circuits underlying the pathophysiology of mood disorders. *Trends Cogn Sci*. 2012;16(1):61–71. doi:10.1016/j.tics.2011.12.011
81. Soares JC, Mann JJ. The anatomy of mood disorders--review of structural neuroimaging studies. *Biol Psychiatry*. 1997;41(1):86–106. doi:10.1016/s0006-3223(96)00006-6
82. Phan KL, Wager TD, Taylor SF, Liberzon I. Functional neuroimaging studies of human emotions. *CNS Spectr*. 2004;9(4):258–266. doi:10.1017/s1092852900009196
83. Qiao L, Wei DT, Li WF, et al. Rumination mediates the relationship between structural variations in ventrolateral prefrontal cortex and sensitivity to negative life events. *Neuroscience*. 2013;255:255–264. doi:10.1016/j.neuroscience.2013.09.053
84. Gotlib IH, Hamilton JP, Cooney RE, et al. Neural processing of reward and loss in girls at risk for major depression. *Arch Gen Psychiatry*. 2010;67(4):380–387. doi:10.1001/archgenpsychiatry.2010.13
85. Hayakawa YK, Sasaki H, Takao H, et al. Structural brain abnormalities in women with subclinical depression, as revealed by voxel-based morphometry and diffusion tensor imaging. *J Affect Disord*. 2013;144(3):263–268. doi:10.1016/j.jad.2012.10.023
86. Adler CM, Adams J, DelBello MP, et al. Evidence of white matter pathology in bipolar disorder adolescents experiencing their first episode of mania: a diffusion tensor imaging study. *Am J Psychiatry*. 2006;163(2):322–324. doi:10.1176/appi.ajp.163.2.322
87. Liu JX, Chen YS, Hsieh JC, et al. Differences in white matter abnormalities between bipolar I and II disorders. *J Affect Disord*. 2010;127(1–3):309–315. doi:10.1016/j.jad.2010.05.026
88. Pompili M, Innamorati M, Mann JJ, et al. Periventricular white matter hyperintensities as predictors of suicide attempts in bipolar disorders and unipolar depression. *Prog Neuropsychopharmacol Biol Psychiatry*. 2008;32(6):1501–1507. doi:10.1016/j.pnpbp.2008.05.009
89. Mahon K, Burdick KE, Szeszko PR. A role for white matter abnormalities in the pathophysiology of bipolar disorder. *Neurosci Biobehav Rev*. 2010;34(4):533–554. doi:10.1016/j.neubiorev.2009.10.012
90. Haznedar MM, Roversi F, Pallanti S, et al. Fronto-thalamo-striatal gray and white matter volumes and anisotropy of their connections in bipolar spectrum illnesses. *Biol Psychiatry*. 2005;57(7):733–742. doi:10.1016/j.biopsych.2005.01.002
91. Zhong S, Wang Y, Lai S, et al. Associations between executive function impairment and biochemical abnormalities in bipolar disorder with suicidal ideation. *J Affect Disord*. 2018;241:282–290. doi:10.1016/j.jad.2018.08.031
92. Zhong S, Wang Y, Zhao G, et al. Similarities of biochemical abnormalities between major depressive disorder and bipolar depression: a proton magnetic resonance spectroscopy study. *J Affect Disord*. 2014;168:380–386. doi:10.1016/j.jad.2014.07.024
93. Frazier JA, Breeze JL, Papadimitriou G, et al. White matter abnormalities in children with and at risk for bipolar disorder. *Bipolar Disord*. 2007;9(8):799–809. doi:10.1111/j.1399-5618.2007.00482.x
94. Wang F, Jackowski M, Kalmar JH, et al. Abnormal anterior cingulum integrity in bipolar disorder determined through diffusion tensor imaging. *Br J Psychiatry*. 2008;193(2):126–129. doi:10.1192/bjp.bp.107.048793
95. Holtzheimer PE, Kelley ME, Gross RE, et al. Subcallosal cingulate deep brain stimulation for treatment-resistant unipolar and bipolar depression. *Arch Gen Psychiatry*. 2012;69(2):150–158. doi:10.1001/archgenpsychiatry.2011.1456

96. Vederine FE, Wessa M, Leboyer M, Houenou J. A meta-analysis of whole-brain diffusion tensor imaging studies in bipolar disorder. *Prog Neuropsychopharmacol Biol Psychiatry*. 2011;35(8):1820–1826. doi:10.1016/j.pnpbp.2011.05.009
97. Gao W, Jiao Q, Qi R, et al. Combined analyses of gray matter voxel-based morphometry and white matter tract-based spatial statistics in pediatric bipolar mania. *J Affect Disord*. 2013;150(1):70–76. doi:10.1016/j.jad.2013.02.021
98. Strakowski SM, Delbello MP, Adler CM. The functional neuroanatomy of bipolar disorder: a review of neuroimaging findings. *Mol Psychiatry*. 2005;10(1):105–116. doi:10.1038/sj.mp.4001585
99. Ishida T, Donishi T, Iwatani J, et al. Elucidating the aberrant brain regions in bipolar disorder using T1-weighted/T2-weighted magnetic resonance ratio images. *Psychiatry Res Neuroimaging*. 2017;263:76–84. doi:10.1016/j.pscychresns.2017.03.006
100. Sani G, Chiapponi C, Piras F, et al. Gray and white matter trajectories in patients with bipolar disorder. *Bipolar Disord*. 2016;18(1):52–62. doi:10.1111/bdi.12359
101. Aylward EH, Roberts-Twillie JV, Barta PE, et al. Basal ganglia volumes and white matter hyperintensities in patients with bipolar disorder. *Am J Psychiatry*. 1994;151(5):687–693. doi:10.1176/ajp.151.5.687
102. Zhang X, Gao W, Cao W, et al. Pallidal volume reduction and prefrontal-striatal-thalamic functional connectivity disruption in pediatric bipolar disorders. *J Affect Disord*. 2022;301:281–288. doi:10.1016/j.jad.2022.01.049
103. Okun MS, Bakay RA, DeLong MR, Vitek JL. Transient manic behavior after pallidotomy. *Brain Cogn*. 2003;52(2):281–283. doi:10.1016/s0278-2626(03)00073-3
104. Pies R. How "objective" are psychiatric diagnoses?: (guess again). *Psychiatry*. 2007;4(10):18–22.
105. Helzer JE, Robins LN, Taibleson M, et al. Reliability of psychiatric diagnosis. I. A methodological review. *Arch Gen Psychiatry*. 1977;34(2):129–133. doi:10.1001/archpsyc.1977.01770140019001
106. Deng F, Wang Y, Huang H, et al. Abnormal segments of right uncinate fasciculus and left anterior thalamic radiation in major and bipolar depression. *Prog Neuropsychopharmacol Biol Psychiatry*. 2018;81:340–349. doi:10.1016/j.pnpbp.2017.09.006
107. Bozhilova N, Welham A, Adams D, et al. Profiles of autism characteristics in thirteen genetic syndromes: a machine learning approach. *Mol Autism*. 2023;14(1):3. doi:10.1186/s13229-022-00530-5